Kinetics of the Partial Oxidation of Methane to Formaldehyde on Silica Catalyst

Francesco Arena
Dipartimento di Chimica Industriale e Ingegneria dei Material, Università degli Studi di Messina, I-98166 S. Agata (Messina) Italy
and
Istituto CNR-TAE, 1-98126 S. Lucia (Messina), Italy

Francesco Frusteri
Istituto CNR-TAE, I-98126 S. Lucia (Messina), Italy

Adolfo Parmaliana
Istituto CNR-TAE, 1-98126 S. Lucia (Messina), Italy
and
Dipartimento di Chimica, Università degli Studi ''La Sapienza,'' 00185, Roma, Italy

The kinetics of the partial oxidation of methane to formaldehyde (MPO) on a ''precipitated'' silica catalyst in the 500–800°C range was investigated. The influence of temperature and reaction mixture composition on the density of reduced sites of the catalyst under steady state was evaluated by in situ reaction temperature oxygen chemisorption measurements. The kinetics of the MPO on silica is pseudo first and zero-order on P_{CH_4} and P_{o_2}, respectively, while the density of reduced sites depends upon the square root of the P_{CH_4}/P_{O_2} ratio. The rate-determining step is the activation of C–H bond of CH_4 molecules ($E_{red} = 142\ kJ \cdot mol^{-1}$), while oxygen replenishment is a nonactivated reaction step ($E_{ox} \approx 20\ kJ \cdot mol^{-1}$). A Langmuir-Hinshelwood kinetic model, accounting for a two-site-dissociative activation mechanism of both CH_4 and O_2, thoroughly describes the steady state of the silica surface and the reaction kinetics of the MPO in the 500–800°C range.

Introduction

The large amount of research interest focused during last decades on the catalytic partial oxidation of methane to oxygenates (MPO) has allowed to ascertain the peculiar functionality of the silica surface in driving the formation of formaldehyde (Brown and Parkyns, 1991; Sun et al., 1992; Parmaliana et al., 1993; Koranne et al., 1994; Parmaliana and Arena, 1997; Arena et al., 1997; Herman et al., 1997). The preparation method markedly affects the performance of bare silica catalysts (Sun et al., 1992; Parmaliana et al., 1993; Arena et al., 1995; Vikulov et al., 1996) according to the following activity scale:

''precipitation > sol-gel > pyrolysis,''

as it determines a different density of strained siloxane bridges likely acting as active sites in the MPO (Sun et al., 1992; Vikulov et al., 1996). Then, as a consequence of marked differences in the reactivity of the silica samples, the addition of promoters might have either a positive or negative effect on the activity of the carrier. In particular, while V_2O_5 promotes the reactivity of any silica samples (Spencer and Pereira, 1989; Kennedy et al., 1992; Kartheuser et al., 1993; Parmaliana et al., 1993, 1994, 1995a,b; Koranne et al., 1993, 1994; Arena et al., 1995). MoO_3 enhances the performance of sol-gel and pyrolitic samples (Spencer and Pereira, 1987; Sun et al., 1992; Mauti and Mims, 1993; Parmaliana et al., 1993, 1995a,b; Arena et al., 1995) depressing that of the precipitated one (Parmaliana et al., 1993; Arena et al., 1995; Parmaliana and Arena, 1997).

Correspondence concerning this article should be addressed to F. Arena.

Although the many attempts to shed light on the nature of the active sites and reaction mechanism, the role of the catalyst lattice oxygen ions (LOI) in the CH_4 activation and HCHO formation processes is still controversial (Kennedy et al., 1992; Kartheuser et al., 1993; Mauti and Mims, 1993; Koranne et al., 1993, 1994; Parmaliana et al., 1993, 1995a,b; Faraldos et al., 1996; Arena et al., 1994, 1997; Herman et al., 1997). In particular, isotopic labeling (Koranne et al., 1993, 1994; Mauti and Mims, 1993) and transient techniques (Kennedy et al., 1992; Kartheuser et al., 1993; Koranne et al., 1993, 1994; Parmaliana et al., 1994, 1995a,b; Arena et al., 1994, 1997; Parmaliana and Arena, 1997) were used to probe the origin (LOI or gas-phase O_2) of oxygen atoms inserted into the reaction products. Yet, the capability of oxygenated compounds to easily undergo the isotopic oxygen exchange with LOI (Koranne et al., 1994; Mauti and Mims, 1993) impeded determination of the origin of the oxygen species directly involved in the MPO reaction. Nevertheless, comparing the reaction rate in the presence and absence of gas-phase oxygen, we argued that the MPO on silica-based catalysts mainly proceeds via a concerted mechanism involving the activation of O_2 on specific reduced sites (ρ) stabilized on the catalyst surface under steady-state conditions (Parmaliana et al., 1994, 1995a,b; Arena et al., 1994, 1997; Parmaliana and Arena, 1997). In fact, direct relationships between reaction rate, HCHO productivity (STY_{HCHO}), and ρ for bare silica samples and diluted (≤ 5 wt %) MoO_3/SiO_2 and V_2O_5/SiO_2 systems were outlined (Parmaliana et al., 1994, 1995). Whereas, the lack of any relationship between reaction rate and ρ for highly loaded (≥ 10 wt %) V_2O_5/SiO_2 catalysts was ascribed to a change in the reaction mechanism from *concerted* to *redox* enabled by the formation of V_2O_5 crystallites on the silica surface, which imply the overreduction of the catalyst surface leading mostly to CO_x (Parmaliana et al., 1994, 1995a,b; Arena et al., 1997). Then all this evidence infers that the oxygen species driving HCHO formation are not related to LOI (Koranne et al., 1994; Parmaliana et al., 1995a,b; Faraldos et al., 1996; Parmaliana and Arena, 1997; Arena et al., 1997). Furthermore, we found that the bare ''precipitated'' silica catalyst (PS) exhibited the best activity-selectivity pattern in MPO in the 600–700°C range (Arena et al., 1994, 1995; Parmaliana et al., 1998). That is, by using a recirculation continuous-flow reactor configuration, we showed that HCHO molar yields of up to 20–22% can be attained on the PS catalyst between 650 and 680°C (Parmaliana et al., 1998).

Earlier kinetic studies of the MPO reaction mostly addressed modeling of the different activity–selectivity pattern of MoO_3/SiO_2 and V_2O_5/SiO_2 systems (Spencer and Pereira, 1987, 1989; Amiridis et al., 1991; Koranne et al., 1994). In particular, Amiridis et al. developed a microkinetic model based on the thermodynamic analysis of the elementary steps, providing a useful tool to describe the macrokinetics of the MPO reaction network on the SiO_2-supported MoO_3 and V_2O_5 catalysts in a wide range of experimental conditions. However, no direct evidence about the stationary state of the catalytic surface under reaction conditions and then no direct structure–activity relationships had been provided before. In this respect, it is recognized that the gas–solid interactions occurring under reaction conditions plays a crucial role in determining the steady state of the catalyst surface, and thus the activity–selectivity pattern of oxide systems in selective oxidation reactions (Sokolovskii, 1990; Bielañski and Haber, 1991; Kasztelan, 1992; Kung, 1992). Then, the development of a formal kinetic model that relates the reaction kinetics with the steady state of the catalyst surface is wanted for predicting the mechanism of the MPO reaction on silica-based oxide systems (Sokolovskii, 1990; Arena et al., 2000).

This article therefore reports a systematic study of the influences of temperature and reaction mixture composition (i.e., P_{CH_4}, P_{O_2}, and P_{CH_4}/P_{O_2} ratio) on both activity and steady state of the PS catalyst in the 500–800°C range.

A formal kinetic model of the MPO reaction, which accounts for the activity data and characterization results of the ''precipitated'' silica catalyst, is proposed.

Experimental

Catalyst

A commercial ''precipitated'' silica sample (Si 4-5P Grade, Akzo product; SA_{BET}, 400 $m^2\ g^{-1}$) was the catalyst investigated.

Catalyst testing

Catalytic data in the MPO reaction at 520 and 650°C were obtained using a quartz-tube linear reaction (ID, 4 mm) operating in batch mode ($V = 1.7$ L) and equipped with an external recycle pump and a liquid product condenser ($T = -5$°C) downstream of the reactor, trapping formaldehyde to prevent its further oxidation (Parmaliana et al., 1993). Tests were performed using 0.050 (650°C) or 1.0 g (520°C) of catalyst (16–25 mesh), and a reaction mixture $He/N_2/CH_4/O_2$ recirculating at the rate of 1000 STP $cm^3 \cdot min^{-1}$ (P_{tot}, 1.71 atm), with P_{CH_4} and P_{O_2} varying between 0.079 and 1.214 and 0.02 and 0.171 atm, respectively. All the gaseous products were analyzed on-line by an HP 5890A gas chromatograph equipped with two columns in series (2.5 m Porapak QS 80/100 and 2.5 m Molecular Sieve 5Å kept at 70°C) connected to a thermal conductivity detector (TCD). The HCHO was cumulatively determined at the end of the runs by GC analysis of the condensed mixture by using a 1.8-m Haysep R 100/120 column kept at 130°C. Under these conditions, C and O mass balances were generally better than 98 to 99%.

Catalyst characterization

The influences of the reaction mixture composition and temperature (500–800°C) on the steady state of the catalyst surface were investigated by reaction temperature oxygen chemisorption (RTOC) measurements, carried out in pulse mode in a continuous-flow apparatus using (*Oxysorb*, Alltech product) O_2-purified He as carrier gas (Parmaliana et al., 1994, 1995a,b). Prior to each oxygen uptake test, the catalyst sample (0.1–0.25 g) was conditioned *in situ* for 30 min in a continuous reaction flow ($He/CH_4/O_2$), keeping the contact time constant (τ, 0.166 s) and varying P_{CH_4} (P_{CH_4}, 0.05–0.80; P_{O_2}, 0.1) and P_{O_2} (P_{O_2}, 0.025–0.40; P_{CH_4} 0.2), respectively. After pretreatment, the catalyst sample was flushed in the He carrier flow ($F_{He} = F_{He/CH_4/O_2}$) and then O_2 pulses ($V_{O_2} = 12.9$ nmol) were injected until saturation. O_2 uptakes were quantified by a TCD connected to a DP 700 Data Processor

(Carlo Erba Instruments), each value of density of reduced sites (ρ, $nmol_o \cdot g^{-1}$) being calculated from the average of at least four measurements (std dev $< \pm 5\%$) assuming a "O_2:ρ = 1:2" chemisorption stoichiometry. The total number of reduced sites (ρ_0, $nmol_o \cdot g^{-1}$) was determined after treating the catalyst with a 2% CH_4/He mixture at 650°C for 45 min.

Results and Discussion

Reaction kinetics (T, 520 and 650°C)

The reaction order of the MPO on the silica catalyst at 520 and 650°C with respect to both P_{CH_4} and P_{O_2} has been evaluated using a batch reactor operating in *ideal* kinetic conditions (CH_4 conversion per pass < 0.1%) (Parmaliana et al., 1993). Further, in order to avoid any kinetic constraint, CH_4 conversion values corresponding to O_2 conversion lower than 20% have been considered for the calculation of kinetic data. Activity data at 520 and 650°C and different P_{CH_4}, P_{O_2}, and P_{CH_4}/P_{O_2} are summarized in Table 1 in terms of hourly CH_4 conversion (%), reaction rate ($\mu mol \cdot s^{-1} \cdot g^{-1}$), and product selectivity (S_x, %) values.

Both P_{CH_4} and P_{O_2} exert a positive influence on reaction rate, though it is evident that the effect of the former is much stronger. That is, according to data in the literature pointing to a *quasi-first* and *quasi-zero* order in CH_4 and O_2 pressure, respectively (Spencer and Pereira, 1987, 1989; Amiridis et al., 1991; McCormick et al., 1997; Alptekin et al., 1999; Arena et al., 2000), reaction orders equal to 1.1 (± 0.1) and 0.9 (± 0.03) on P_{CH_4} and 0.2 (± 0.06) on P_{O_2} at 520 and 650°C, respectively, have been found. Then, in the 520–650°C range, the following power-law rate equation can be written for the MPO on silica:

$$Rate_{CH_4} = k_{exp} \cdot P_{CH_4} \cdot P_{O_2}^{0.2}. \quad (1)$$

Furthermore, the peculiar operation mode of the batch reactor, running at constant methane conversion per pass (0.065–0.07%) and ensuring HCHO separation from the reaction stream, implies that neither temperature nor the P_{CH_4}/P_{O_2} ratio significantly affects the S_{HCHO} (67–76%). Thus, considering that CO and CO_2 arise from the consecutive oxidation of HCHO and CO, respectively (Arena et al., 1995; Parmaliana and Arena, 1997), the CO_x distrbution signifies that the surface catalyzed oxidation of HCHO to CO (S_{CO}, 10–28%) occurs at a much higher rate than that of oxidation of CO to CO_2 (S_{CO_2}, 5–21%); this last reaction, however, is more likely to occur at 520°C (such as $K_{520°C}/K_{650°C} \cong 3 \cdot 10^4$).

Reaction mixture composition and density of reduced sites (T_R = 650°C)

Since we previously found that the activity of the MPO catalysts is directly related to their capability to stabilize surface reduced sites, which, acting as O_2 activation centers, ensure the occurrence of the redox cycle under steady-state conditions (Parmaliana et al., 1994, 1995a,b; Arena et al., 1994, 1997; Arena et al., 2000), the influence of the concentration of CH_4 and O_2 on the steady state of the silica surface at 650°C has been evaluated by a series of RTOC measurements at different P_{CH_4}, P_{O_2}, and P_{CH_4}/P_{O_2}. The values of the absolute density of the reduced sites (ρ, $nmol_o \cdot g^{-1}$), the total number of reducible sites (ρ_0, $nmol_o \cdot g^{-1}$), and the fractional density of the reduced sites (θ_{red}, ρ/ρ_0) are listed in Table 2.

The total concentration of reducible sites (ρ_0) equals to 373.63 $nmol_o \cdot g^{-1}$, while when gas-phase O_2 is present, the density of reduced sites (ρ) drops considerably ($\rho < 65 nmol_o \cdot g^{-1}$). In particular, it is evident that ρ is almost unaffected by the absolute values of P_{CH_4} and P_{O_2}, depending only upon the P_{CH_4}/P_{O_2} ratio ($P_{CH_4}/P_{O_2} = 0.5$, $\rho \approx 15$ $nmol_o \cdot g^{-1}$; $P_{CH_4}/P_{O_2} = 8$, $\rho \approx 64$ $nmol_o \cdot g^{-1}$). The opposite trends, θ_{red} with P_{CH_4} and P_{O_2}, are depicted in Figure 1A, while plotting

Table 1. Activity Data (batch reactor) of the Silica Catalyst at 520 and 650°C*

P_{CH_4} (atm)	P_{O_2} (atm)	P_{CH_4}/P_{O_2}	Hourly CH_4 Conv. (%)	Rate ($\mu mol_{CH_4} \cdot s^{-1} \cdot g^{-1}$)	S_{HCHO}	S_{CO} (%)	S_{CO_2} (%)
			T_R = 520°C				
0.342	0.023	14.7	2.7	0.13	67	15	18
0.342	0.039	8.8	3.1	0.16	69	10	21
0.342	0.171	2.0	3.3	0.20	76	13	11
0.082	0.171	0.5	2.1	0.03	73	10	17
0.174	0.171	1.0	2.4	0.06	72	15	13
0.342	0.171	2.0	3.3	0.20	76	13	11
0.705	0.171	4.1	4.2	0.41	73	18	9
0.905	0.171	5.3	4.1	0.52	68	28	4
1.187	0.171	7.6	3.5	0.58	70	26	4
			T_R = 650°C				
0.342	0.020	17.0	2.2	2.09	75	20	5
0.342	0.044	7.8	2.9	2.76	73	22	5
0.342	0.171	2.0	3.5	3.33	76	19	5
0.079	0.171	0.5	4.5	0.98	74	20	6
0.162	0.171	1.0	4.3	1.94	70	22	8
0.342	0.171	2.0	3.5	3.33	76	19	5
0.674	0.171	4.0	3.4	6.36	74	20	6
0.973	0.171	5.8	3.7	10.00	71	20	9
1.214	0.171	7.6	3.2	10.79	71	23	6

*Includes influence of P_{CH_4}, P_{O_2}, and P_{CH_4}/P_{O_2} on reaction rate and product selectivity.

Table 2. Absolute (ρ) and Fractional Density of Reduced Sites (θ_{red}) of the Silica Catalyst at 650°C*

P_{CH_4}/P_{O_2}	P_{CH_4} (atm)	P_{O_2} (atm)	ρ ($nmol_o \cdot g^{-1}$)	θ_{red}
0.5	0.05	0.10	14.95	0.04
0.5	0.20	0.40	14.95	0.04
1.0	0.10	0.10	23.25	0.064
1.0	0.20	0.20	23.25	0.064
2.0	0.20	0.10	29.90	0.08
4.0	0.10	0.025	43.18	0.115
4.0	0.20	0.05	46.50	0.124
4.0	0.40	0.10	43.18	0.115
6.0	0.60	0.10	53.14	0.142
8.0	0.20	0.025	64.76	0.173
8.0	0.80	0.10	63.10	0.169
∞	0.02	0.00	373.63**	1.00

*Includes influence of the P_{CH_4}, P_{O_2}, and P_{CH_4}/P_{O_2}.
**ρ_0 value attained after 45 min treatment time.

the ln θ_{red} vs. ln P_{CH_4} and ln P_{O_2}, two inverse linear relationships are obtained, as shown in Figure 1B. Linear regression analysis of such correlations indicate a half (0.509 ± 0.03) and a negative-half (-0.501 ± 0.02) order dependence of θ_{red} upon P_{CH_4} and P_{O_2}, respectively, thus pointing to the redox potential of the reaction atmosphere (i.e., P_{CH_4}/P_{O_2}) as the factor controlling the steady state of the catalyst surface (Bielañski and Haber, 1991; Kung, 1992; Arena et al., 2000). The dependence of the reaction kinetics on P_{CH_4} and P_{O_2} (Eq. 1) thus reflects a rise in the *sticking* frequency of CH_4 and O_2 molecules on the active sites of the silica surface.

Reduced sites equation model

The half-order dependence of θ_{red} on the P_{CH_4}/P_{O_2} ratio is evidently diagnostic of a *two-site* dissociative activation of both CH_4 and O_2 molecules on the same active sites (competitive) of the silica surface. Thus, if the lifetime of the adsorbed intermediate(s) is negligible with respect to the rate of transformation into reaction products in the T range investigated (Amiridis et al., 1991; Bielañski and Haber, 1991; Kung, 1992; Sun et al., 1992; Koranne et al., 1993, 1994; Herman et al., 1997; Arena et al., 2000), the occurrence of the following irreversible surface reactions is inferred:

$$CH_4 + 2\rho\text{-}O \rightarrow HCHO + H_2O + 2\rho \quad \text{(i)}$$

$$O_2 + 2\rho \rightarrow 2\rho\text{-}O, \quad \text{(ii)}$$

where "ρ" and "ρ-O" represent the reduced and oxidized form, respectively, of the active sites. At the steady state, considering the mass balance on the active sites ($[\rho] + [\rho\text{-}O] = [\rho_0]$) we obtain the following rate equation:

$$\text{Rate}_{red} = k_{red} \cdot P_{CH4} \cdot (\rho_0 - \rho)^2 \quad (2)$$

for the formation of reduced sites (Rate_{red}). Being negligible, the rate of diffusion of O^{2-} ions across the silica lattice under MPO conditions (Sun et al., 1992; Koranne et al., 1994; Parmaliana et al., 1994, 1995a,b; Arena et al., 1997), at the steady state the rate at which the reduced sites disappear equals that of catalyst oxidation (Rate_{ox}):

$$\text{Rate}_{ox} = k_{ox} \cdot P_{O_2} \cdot \rho^2. \quad (3)$$

Further, considering the relationship between ρ and ρ_0,

$$\rho = \rho_0 \cdot \theta_{red}, \quad (4)$$

with $0 \le \theta_{red} \le 1$ representing the fractional density of the reduced sites, at steady state Eqs. 2 and 3 must equal

$$k_{ox} \cdot P_{O_2} \cdot \rho_0^2 \cdot \theta_{red}^2 = k_{red} \cdot P_{CH_4} \cdot \rho_0^2 \cdot (1 - \theta_{red})^2. \quad (5)$$

Solving for θ_{red}, the following equation for the density of the reduced sites as a function of P_{CH_4} and P_{O_2} is obtained:

$$\theta_{red} = \frac{\sqrt{\frac{k_{red}}{k_{ox}}} \cdot \left(\frac{P_{CH_4}}{P_{O_2}}\right)^{0.5}}{1 + \sqrt{\frac{k_{red}}{k_{ox}}} \cdot \left(\frac{P_{CH_4}}{P_{O_2}}\right)^{0.5}}. \quad (6)$$

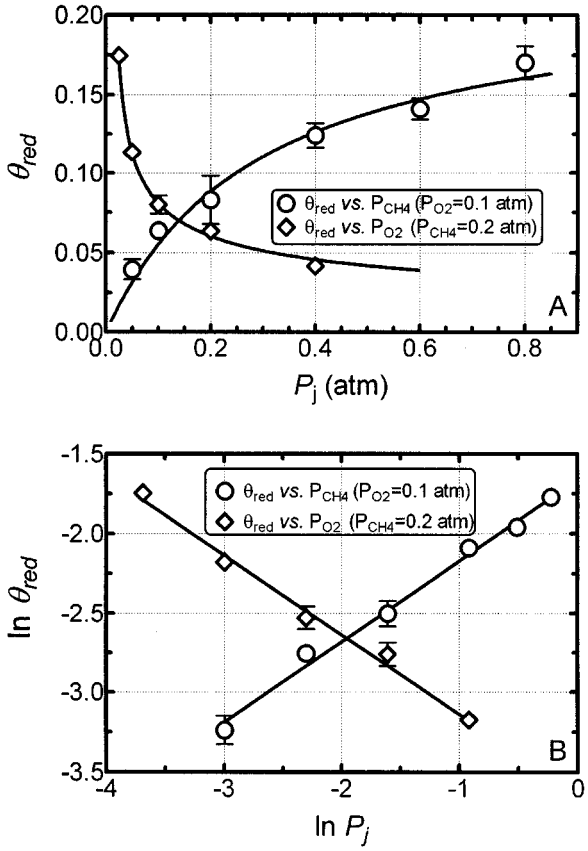

Figure 1. Partial oxidation of methane to formaldehyde on silica catalyst (T = 650°C).

(A) Influence of P_{CH_4} and P_{O_2} on the fractional density of reduced sites (θ_{red}); (B) log-plot of θ_{red} vs. P_{CH_4} and P_{O_2}.

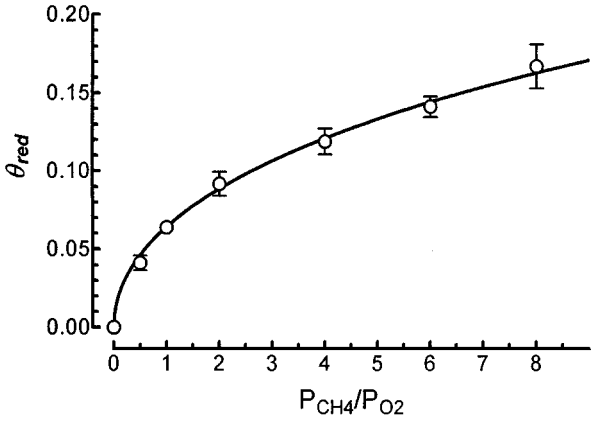

Figure 2. Partial oxidation of methane to formaldehyde on silica catalyst ($T = 650°C$).

Curve fitting of "θ_{red} vs. P_{CH_4}/P_{O_2}" RTOC data by Eq. 6.

Apparently, such a relationship matches the experimental dependence of θ_{red} on the square root of the P_{CH_4}/P_{O_2} ratio if $[(k_{red}P_{CH_4}/k_{ox}\ P_{O_2})^{0.5}] \ll 1$. In fact, the preceding equation, which is analogous to the Langmuir-Hinshelwood (L-H) dissociative adsorption model, but with the P_{CH_4}/P_{O_2} ratio instead of the P_j term, provides a very accurate fitting ($r^2 \cong 0.99$) of the RTOC data as a function of P_{CH_4}/P_{O_2}, as shown in Figure 2. Nonlinear regression analysis of this curve indicates a value of the k_{red}/k_{ox} ratio equal to 0.00473, which, for $P_{CH_4}/P_{O_2} \leq 8$, practically confirms the empirical dependence of θ_{red} upon $\sqrt{(P_{CH_4}/P_{O_2})}$.

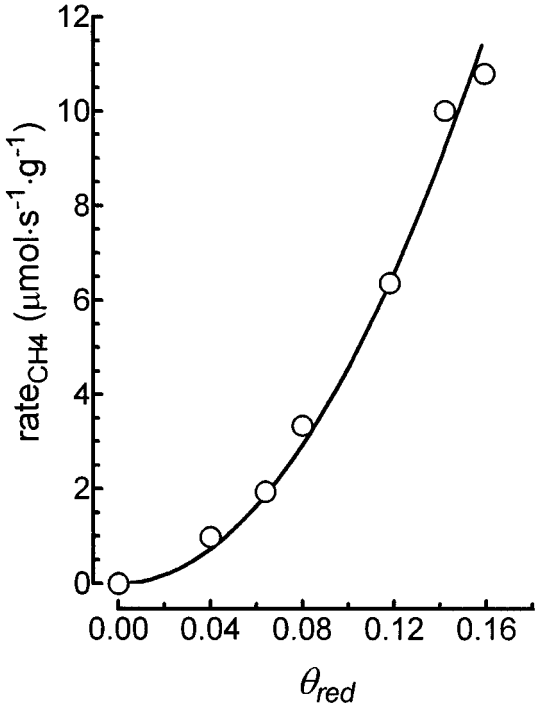

Figure 3. Partial oxidation of methane to formaldehyde on silica catalyst ($T = 650°C$).

2nd-order relationship between reaction rate and θ_{red}.

Kinetic modeling of the MPO on silica catalyst

According to the kinetic dependence of the reaction rate upon P_{CH_4} and P_{O_2}, respectively (Eq. 1), indicating the C–H bond activation in CH_4 molecules as the *rate-determining step* (rds) of the MPO on the silica catalyst (Spencer and Pereira, 1987, 1989; Amiridis et al., 1991; Arena et al., 1994, 1997; Alptekin et al., 1999), RTOC data (k_{red}/k_{ox}, 0.00473) point to a rate of catalyst oxidation much faster than that of reduction (Kartheuser et al., 1993; Arena et al., 1994, 1997; McCormick et al., 1997; Arena et al., 2000).

Furthermore, Eq. 6, which constitutes the basis of the kinetic model of the MPO reaction on the silica catalyst, allows to address the origin of the empirical power-law rate equation (Eq. 1). That is, since reactions denoted by k_{red} (Eq. i) and k_{ox} (Eq. ii) are irreversible, the overall rate of methane conversion ($Rate_{CH_4}$) at the steady state equals that of catalyst reduction (Eq. 2) and oxidation (Eq. 3):

$$Rate_{CH_4} = k_{ox} \cdot P_{O_2} \cdot \rho_0^2 \cdot \theta_{red}^2 = k_{red} \cdot P_{CH_4} \cdot \rho_0^2 \cdot (1 - \theta_{red})^2, \quad (7)$$

which suggests a second-order relationship between the reaction rate and θ_{red}, as shown in Figure 3. Then, substituting Eq. 6 for θ_{red} in Eq. 7, the following rate equation is obtained:

$$Rate_{CH_4} = \rho_0^2 \cdot \frac{k_{red} \cdot P_{CH_4}}{\left(1 + \sqrt{\dfrac{k_{red} \cdot P_{CH_4}}{k_{ox} \cdot P_{O_2}}}\right)^2} \quad (8)$$

Taking the dissociative activation of O_2 and CH_4 into account, the preceding rate equation matches the kinetic model of selective oxidation reactions that occur by a *redox mechanism* on oxide systems that have a negligible rate of lattice oxygen diffusion (Bielañski and Haber, 1991; Kasztelan, 1992; Kung, 1992), since, according to our earlier findings (Arena et al., 1994, 1997; Parmaliana et al., 1994, 1995a,b; Arena et al., 2000), the model predicts a reaction rate close to zero in the absence of gas-phase O_2 (such as $P_{CH_4}/P_{O_2} \to \infty$). In addition, the rate equation confirms that, at high values of the P_{CH_4}/P_{O_2} ratio, the reaction order of the MPO on P_{CH_4} becomes lower than one since the catalyst surface becomes more reduced, which leads to a decrease in the concentration of sites (ρ-O) catalyzing CH_4 activation (McCormick et al., 1997; Alptekin et al., 1999; Arena et al., 2000). That is, according to Bielañski and Haber, this infers that the MPO on silica catalyst proceeds according to a *push–pull*, or *concerted mechanism*, with a CH_4 activation rate much slower (RDS) than that of O_2 incorporation (Arena et al., 1997, 2000).

Kinetic model vs. experimental data ($T = 650°C$)

Nonlinear regression analysis of the curve shown in Figure 3 yielded values of k_{ox} and k_{red} equal to 1.9×10^{10} and 9.0×10^7 $g \cdot mol^{-1} \cdot s^{-1} \cdot atm^{-1}$, respectively ($k_{red}/k_{ox}$, 0.00473). These values were used to calculate reaction rate values at different P_{CH_4}, P_{O_2}, and P_{CH_4}/P_{O_2}, which are compared with experimental data (Table 1) in Figure 4. The good agreement between experimental and calculated data is the most relevant proof of the reliability of the kinetic model, though Eqs.

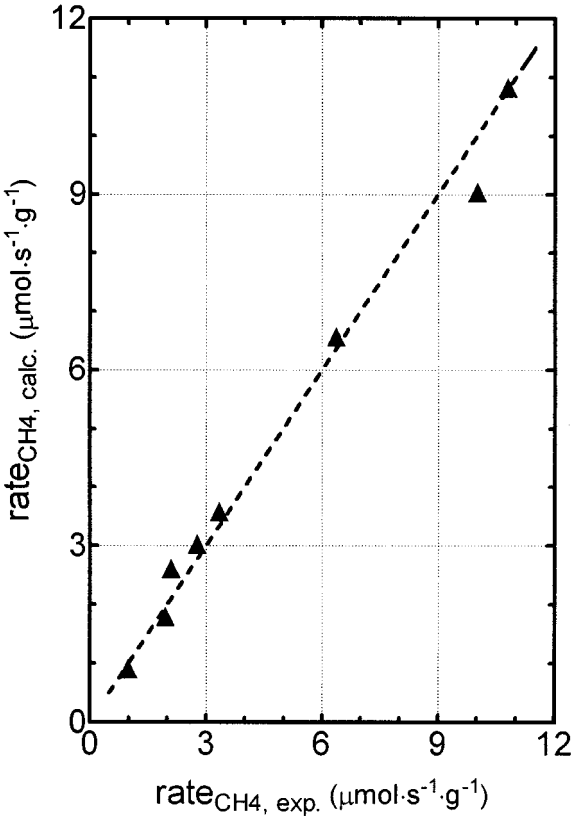

Figure 4. Partial oxidation of methane to formaldehyde on silica catalyst ($T = 650$°C).

Calculated vs. experimental (Table 1) reaction-rate values.

6 and 8 depend on the assumption of a full conversion of methane to formaldehyde (Eq. i). On the other hand, the catalytic nature of the consecutive oxidation of HCHO to CO and CO_2 (Spencer and Pereira, 1989; Amiridis et al., 1991; Arena et al., 1995) implies that the mass balance of surface oxygen atoms is also a function of product selectivity (Bielañski and Haber, 1991; Kung, 1992). That is, disregarding the transformation of CO into CO_2 as this reaction proceeds with a significantly slower rate (see Table 1), only the consecutive oxidation of HCHO will be taken into account:

$$HCHO + \rho\text{-}O \rightarrow CO + H_2O + \rho. \qquad \text{(iii)}$$

This means that the overall rate of oxygen consumption is related to that of methane conversion by the following relationship:

$$\text{Rate}_{O_2} = \text{Rate}_{CH_4} \cdot n = \text{Rate}_{CH_4} \cdot (S_{HCHO} \times f_{HCHO} + S_{CO} \times f_{CO}), \quad (9)$$

where n is equal to $(S_{HCHO} \times f_{HCHO} + S_{CO} \times f_{CO})$ and f_{HCHO} and f_{CO} represent the stoichiometric factors of HCHO and CO formation, equal to 1.0 and 1.5 respectively.

At the steady state, Eq. 6 thus becomes

$$\theta_{red} = \frac{\sqrt{\frac{n \cdot k_{red}}{k_{ox}}} \cdot \left(\frac{P_{CH_4}}{P_{O_2}}\right)^{0.5}}{1 + \sqrt{\frac{n \cdot k_{red}}{k_{ox}}} \cdot \left(\frac{P_{CH_4}}{P_{O_2}}\right)^{0.5}}. \qquad (10)$$

Considering that under continuous flow conditions (RTOC) roughly an equimolar selectivity to HCHO and CO is attained at 650°C for $\tau = 0.166$ sec (Arena et al., 1995), and that the product selectivity ($S_{HCHO} = S_{CO} = 50\%$) would not vary significantly for a P_{CH_4}/P_{O_2} ratio ranging between 0.5 and 8, Eq. 10 signals that θ_{red} under continuous-flow conditions should be slightly larger than that stabilized on the silica surface in the batch reactor because of the lower CO selectivity (approximately 30%). Thus, a larger rate of O_2 consumption implies that k_{ox} really must be multiplied by a factor of 1.25 (such as n under continuous flow (RTOC) reaction conditions), which results in R_{ox} equal to 2.4×10^{10} g·mol^{-1}s^{-1} atm^{-1} ($k_{red}/k_{ox} = 0.378$). A comparison of "θ_{red} vs. P_{CH_4}/P_{O_2}" curves, obtained from Eqs. 6 ($S_{HCHO} = 1.0$) and 10 ($S_{CO} = 0.3$ and $S_{CO} = 0.5$ in the batch and continuous-flow reactors, respectively) on the basis of the actual values of k_{red} (9.0×10^7 g·mol^{-1}·s^{-1}·atm^{-1}) and k_{ox} (2.4×10^{10} g·mol^{-1}·s^{-1}·atm^{-1}) is outlined in Figure 5. It can be seen that the different values of the $[n \cdot (k_{red}/k_{ox})]$ term affect only slightly θ_{red}, and deviations practically lie within the intrinsic uncertainty of RTOC measurements. Furthermore, taking Eq. 10 into account, the rate equation becomes

$$\text{Rate}_{CH_4} = \rho_0^2 \cdot \frac{k_{red} \cdot P_{CH_4}}{\left(1 + \sqrt{\frac{n \cdot k_{red}}{k_{ox}}} \cdot \left(\frac{P_{CH_4}}{P_{O_2}}\right)^{0.5}\right)^2}. \qquad (11)$$

Besides depending on P_{CH_4} and P_{CH_4}/P_{O_2}, this expression signals that the reaction rate is also inversely related to CO_x selectivity (Arena et al., 2000). From a physical point of view,

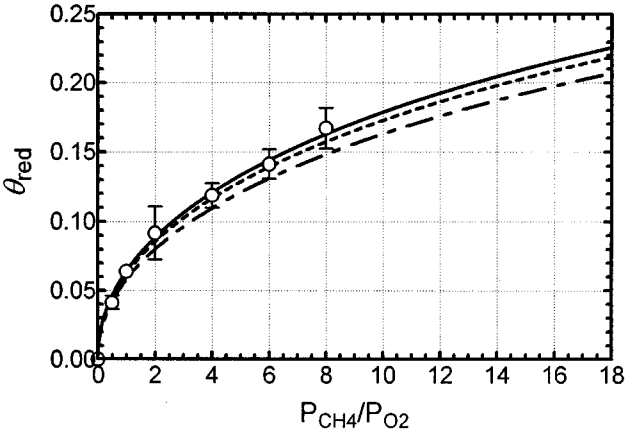

Figure 5. Partial oxidation of methane to formaldehyde on silica catalyst ($T = 650$°C).

"θ_{red} vs. P_{CH_4}/P_{O_2}" curves as a function of the product selectivity.

Legend: (——) $S_{HCHO} = 100\%$; (·—·—·) $S_{HCHO} = 70\%$ (batch reactor data); (– – –) $S_{HCHO} = 50\%$ (continuous flow (RTOC) reactor data).

Table 3. CH_4 and O_2 Conversion and Product Selectivity vs. Reaction Time at 650°C

Time (min)	CH_4 Conv. (%)	(%)	O_2 Conv. (%)	S_{HCHO} (%)	S_{CO} (%)	S_{CO_2} (%)
26	1.25		3.10	73	24	3
49	2.61		6.12	75	21	4
71	4.05		9.00	76	20	4
94	5.22		11.93	75	20	5
116	6.78		15.07	76	19	5
139	7.95		18.11	75	19	6
162	9.46		21.16	76	19	5
184	10.69		24.42	75	19	6
207	12.15		27.37	75	19	6
229	13.51		30.40	75	19	6
251	14.75		33.43	75	19	6
274	16.07		36.50	75	18	7
297	17.37		39.42	75	18	7
319	18.78		42.43	75	18	7
341	19.94		45.47	75	18	7
363	21.10		48.32	75	18	7
385	22.45		51.21	75	17	8
408	23.61		54.03	75	17	8
431	24.81		56.84	74	17	9
519	29.33		67.27	74	17	9
585	32.22		74.14	74	17	9
651	34.93		80.44	74	16	10
1098	43.14		99.87	74	15	11

this infers that an increase in $S_{CO} + S_{CO_2}$ yields a (slightly) deeper reduction of the silica surface, which, however, reflects negligible changes in reaction rate. In fact, considering the low values of the k_{red}/k_{ox} ratio in the whole 500–800°C range (see *infra* Table 4), it is evident that the reliability of the kinetic model is practically unaffected, even by marked changes in the product distribution.

On the other hand, at high values of the P_{CH_4}/P_{O_2} ratio, the increasing weight of the inhibition factor accounts for the kinetic dependence of the MPO reaction on P_{O_2} (0.2). This is very evident when integral BR kinetic data at 650°C and $P_{CH_4}/P_{O_2} = 2$, summarized in Table 3, are compared to the first- and zero-order kinetic law on P_{CH_4} and P_{O_2}, respectively and to the rate equation (Eq. 11).

Thus, taking into account that at any time (t) P_{O_2} is related to P_{CH_4} by the following relationship:

$$P_{O_2} = P_{O_2,in} \cdot \left[1 - n \cdot \frac{P_{CH_4,in}}{P_{O_2,in}} \cdot \left(\frac{P_{CH_4,in} - P_{CH_4}}{P_{CH_4,in}}\right)\right] = n \cdot P_{CH_4} - \left(n \cdot P_{CH_4,in} - P_{O_2,in}\right), \quad (12)$$

with n having the known meaning related to the product selectivity (Table 3), and in this case equal to 1.155 ($0.75 \times 1 + 0.19 \times 1.5 + 0.06 \times 2 = 1.155$) while $P_{CH_4,in}$ and $P_{O_2,in}$ are the initial ($t = 0$) methane and oxygen pressure, respectively, the following integral,

$$\int_{P_{CH_4,in}}^{P_{CH_4}} \left(1 + \sqrt{\frac{n \cdot k_{red}}{k_{ox}} \cdot \frac{P_{CH_4}}{n \cdot P_{CH_4} - \left(n \cdot P_{CH_4,in} - Pr_{O_2,in}\right)}}\right)^2 \frac{dP_{CH_4}}{P_{CH_4}} = \int_0^t \rho_0^2 \cdot k_{red} \cdot dt \quad (13)$$

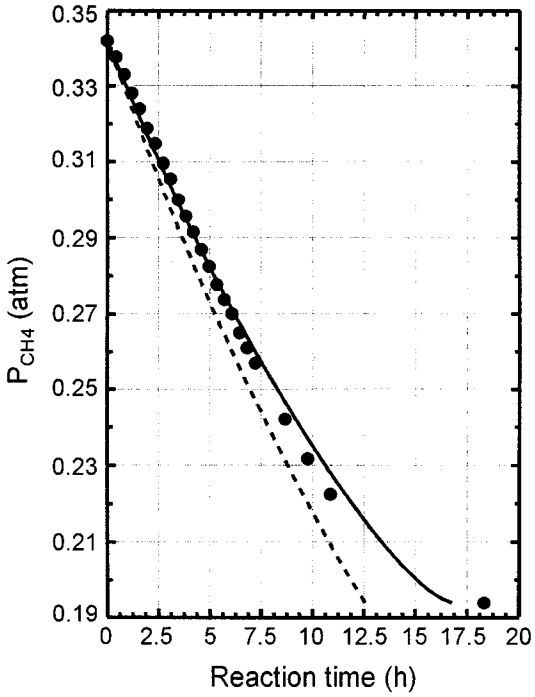

Figure 6. Integral batch-reactor data of the MPO on silica catalyst ($T = 650$°C; $P_{CH_4} = 0.342$ atm; $P_{O_2} = 0.171$ atm).

Curve fitting of experimental data by a 1st-order kinetic law (– – –) and by the kinetic model, Eq. 16 (——).

must be solved to attain the analytical conversion-time curve. Integrating the two terms of Eq. 13 separately, Eq. 14 is obtained:

$$\ln\frac{P_{CH_4,in}}{P_{CH_4}} + \frac{k_{red}}{k_{ox}} \cdot \ln\frac{\left(P_{CH_4,in} - \frac{a}{n}\right)}{\left(P_{CH_4} - \frac{a}{n}\right)} + 2\sqrt{\frac{k_{red}}{k_{ox}}} \cdot \ln\frac{\left[\left(P_{CH_4,in} - \frac{a}{2n}\right) + \sqrt{\left(P_{CH_4,in} - \frac{a}{2n}\right)^2 - \frac{a^2}{4n^2}}\right]}{\left[\left(P_{CH_4} - \frac{a}{2n}\right) + \sqrt{\left(P_{CH_4} - \frac{a}{2n}\right)^2 - \frac{a^2}{4n^2}}\right]} = \left(\rho_0^2 \cdot k_{red}\right) \cdot t, \quad (14)$$

where a is equal to the constant ($n \cdot P_{CH_4,in} - P_{O_2,in}$). Imposing an approximate value for the kinetic constant equal to $1.26 \cdot 10^{-5}$ mol·s^{-1}·g^{-1}, as obtained from the derivative rate equations, the reliability of the two kinetic models in predicting experimental data (Table 3) can be observed in Figure 6. Although the first-order curve partially applies to the experimental data at low CH_4 conversion ($< 5\%$), it is evident that this model cannot account for the observed decay in the reaction rate when marked changed in the reaction mixture composition, mostly linked to the strong decrease in P_{O_2}, occur. This implies that there is an increasing distance between experimental and predicted P_{CH_4} values which becomes very

Table 4. Reaction Rate, Absolute (ρ) and Fractional Density of Reduced Sites (θ_{red}), k_{red}/k_{ox}, and TOF Values in the 500–800°C Range

T_R (°C)	Rate* ($\mu mol_{CH_4} \cdot s^{-1} \cdot g^{-1}$)	ρ ($nmol_o \cdot g^{-1}$)	θ_{red}	k_{red}/k_{ox}	TOF (s^{-1})
500	0.07	6.31	0.0169	1.49×10^{-4}	11.1
520	0.12	8.22	0.0220	2.55×10^{-4}	14.6
550	0.30	11.62	0.0311	5.20×10^{-4}	24.8
600	1.10	19.91	0.0533	1.59×10^{-3}	55.2
650	3.00	31.05	0.0831	47.3×10^{-3}	96.6
700	7.90	49.81	0.1333	1.18×10^{-2}	158.6
725	11.50	59.78	0.1600	18.2×10^{-2}	192.4
750	18.30	74.73	0.2000	2.51×10^{-2}	244.9
800	33.10	112.9	0.3022	4.55×10^{-2}	293.2

*Data from temperature programmed reaction measurements [Arena et al., 1995]: experimental conditions: $P_{H_e}/P_{CH_4}/P_{O_2}$, 7/2/1; F = 50 stp $cm^3 \cdot min^{-1}$: W_{cat}, 0.05 g.

high ($\simeq$ 50%) at the highest level of CH_4 conversion (Figure 6). While Eq. 14, which accounts fully for any changes in the reaction mixture composition, very accurately fits all the experimental data (Figure 6), the maximum distance between predicted and experimental values being as high as 5–6% in the whole range of CH_4 (0–43%) and O_2 (0–99%) conversion.

The Influence of T on the kinetic parameters and activation energy of the reaction steps

Reaction-rate data, taken from an earlier temperature programmed reaction study (Arena et al., 1995), and the experimental values of ρ, θ_{red}, the k_{red}/k_{ox} ratio, and turnover frequency (TOF), defined as the ratio between reaction rate and concentration of unreduced sites (i.e., TOF (s^{-1}) = rate/[ρ-O] = rate/[$\rho_0 \cdot (1 - \theta_{red})$]), of the SiO_2 catalyst in the 500–800°C range at $P_{CH_4}/P_{O_2} = 2$, are summarized in Table 4. Using such data in an Arrhenius plot, as shown in Figure 7, excellent linear correlations prove the occurrence of the main reaction pathway in the range of temperature spanned (Sun et al., 1992; Parmaliana and Arena, 1997). Thus, the apparent activation energy (E_{app}) of the MPO reaction on silica, already taken from the activity data reported in Table 4 (Parmaliana and Arena, 1997), is equal to 142 ± 8 kJ·mol^{-1}, while E_{red}, E_{ox}, E_0, and E_{TOF} are equal to 159, 20, 67 and 148 kJ·mol^{-1}, respectively. To highlight the origin of these E values, the following mathematical relationships from model Eqs. 10 and 11 should be taken into account:

$$d(\ln \text{rate})/d(1/T) = -E_{app}/R \quad (15)$$

$$d(\ln \text{rate})/d(1/T) = -E_{red}/R + 2\,d\left\{\ln\left[\left(1+\sqrt{n}\cdot(k_{red}/k_{ox})\right]\right\}/d(1/T) \quad (16)$$

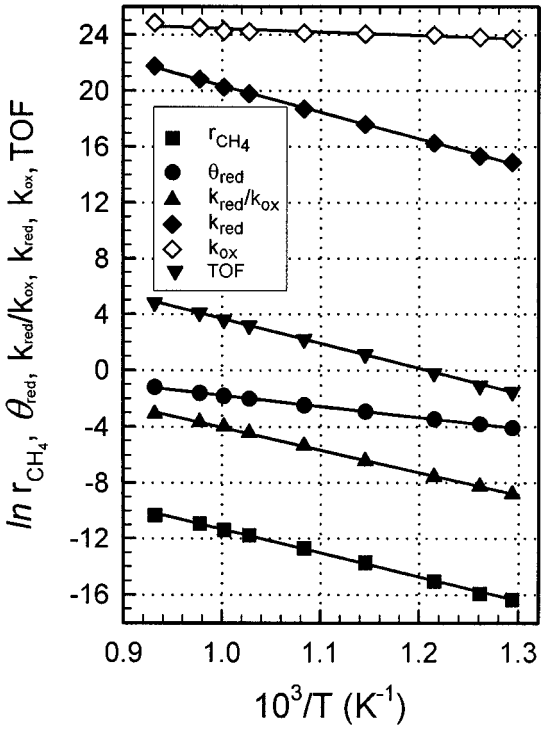

Figure 7. Arrhenius plot of the MPO reaction steps (T range, 500–800°C).

$$d(\ln \text{TOF})/d(1/T) = -E_{red}/R + d\left\{\ln\left[\left(1+\sqrt{n}\cdot(k_{red}/k_{ox})\right]\right\}/d(1/T) \quad (17)$$

$$d(\ln \theta_{red})/d(1/T) = -1/2\,E_{red}/R + 1/2\,E_{ox}/R + d\left\{\ln\left[\left(1+\sqrt{n}\cdot(k_{red}/k_{ox})\right]\right\}/d(1/T). \quad (18)$$

Disregarding the effects of the changes in product selectivity (see earlier), and considering that the k_{red}/k_{ox} ratio is always much less than unit in the whole range of T (Table 4), it is evident that the correction factor "$\ln[(1+\sqrt{n}\cdot(k_{red}/k_{ox})]$ is nearly always negligible (e.g., 0.012 at 500°C and 0.193 at 800°C) in the computation of E values. Then, calculated and experimental data on activation energies, as compared in Table 5, show an absolute agreement between measured and predicted E values, which also provides evidence of the process of O_2 replenishment as a *nonactivated* reaction step ($E_{ox} \approx 0$). This evidence, coupled with the full agreement between experimental (Tables 1 and 4) and calculated reaction-rate values at different T, P_{CH_4}, and P_{O_2}, as shown in Figure 8, prove both the physico-chemical consistency of our kinetic

Table 5. Activation Energy (E) of MPO Reaction Steps: Model vs. Experimental Data

Reaction Step	E Notation	Model Value	Exp. Value (kJ·mol^{-1})
$CH_4 + O_2 \rightarrow$ products	E_{app}	$\cong E_{red}$	142 ± 8
$CH_4 + 2\rho - O \rightarrow$ products $+ 2\rho$	E_{red}	E_{red}	159 ± 8
$2\rho + O_2 \rightarrow 2\rho - O$	E_{ox}	—	20 ± 10
$\rho - O + CH_4 \rightarrow \rho$	E_θ	$\cong 1/2\,E_{red} - 1/2\,E_{ox}$	67 ± 8
rate/[$\rho - O$]	E_{TOF}	$\cong E_{red}$	148 ± 9

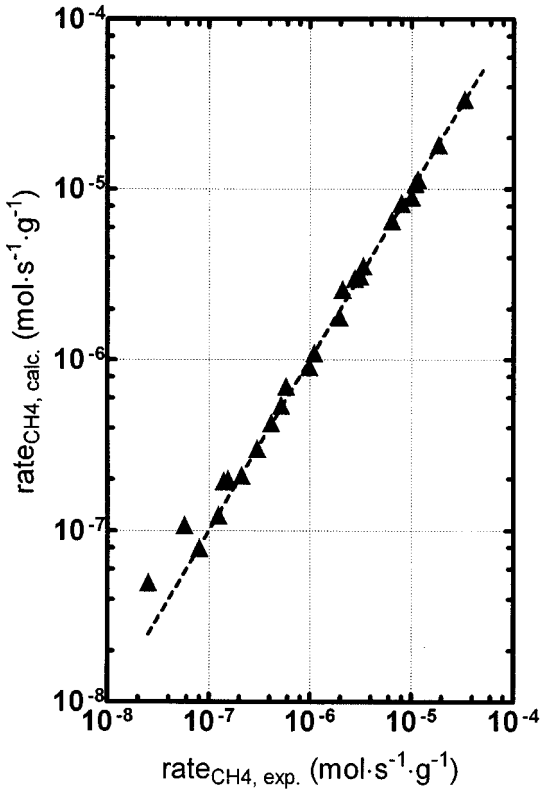

Figure 8. Partial oxidation of methane to formaldehyde on silica catalyst (*T* range, 500–800°C).

Calculated vs. experimental (Tables 1 and 4) reaction rate values at different T, P_{CH_4} and P_{O_2}.

model and its general validity in accounting for the kinetics of the MPO on the silica catalyst.

Conclusions

The kinetics of the partial oxidation of methane to formadehyde on the ''precipitated'' silica in the 500–800°C range have been investigated and thoroughly linked with the steady state of the catalyst surface.

Thus, the main results of this work can be summarized as follows:

- The density of reduced catalyst sites under steady-state conditions depends upon the square-root of the P_{CH_4}/P_{O_2} ratio;
- A Langmuir–Hinshelwood reaction model accounts for the *two-sites surface activation* of both CH_4 and O_2 molecules successfully predicting the kinetics of the MPO on the precipitated SiO_2 catalyst in the 500–800°C range;
- The RDS of the MPO reaction on silica is the activation of the C–H bond in methane molecules, while the O_2 replenishment is a nonactivated reaction step ($E_{ox} \approx 0$).

Acknowledgments

The present work is a part of a project coordinated by Prof. A Zecchina and cofinanced by the Italian M.U.R.S.T. (COFIN 98, AREA 03).

Notation

P_{CH_4}, P_{O_2} = absolute pressure of methane and oxygen, atm
E_{red} = activation energy of the CH_4 activation step, kJ·mol^{-1}
E_{ox} = activation energy of the O_2 activation step, kJ·mol^{-1}
R = universal constant of gas, J·mol^{-1}·K^{-1}

Literature Cited

Alptekin, G. O., A. M. Herring, D. L. Williamson, T. R. Ohno, and R. L. McCormick, ''Methane Partial Oxidation by Unsupported and Silica Supported Iron Phosphate Catalysts,'' *J. Catal.*, **181**, 104 (1999).

Amiridis, M. D., J. E. Rekoske, J. A. Dumesic, D. F. Rudd, N. D. Spencer, and C. J. Pereira, ''Simulation of Methane Partial Oxidation over Silica-Supported MoO_3 and V_2O_5,'' *AIChE J.*, **37**, 87 (1991).

Arena, F., F. Frusteri, D. Miceli, A. Parmaliana, and N. Giordano, ''Mechanistic Evidences of the Partial Oxidation of Methane to Formaldehyde over Silica Based Oxide Catalysts by Temperature Programmed Reaction Studies,'' *Catal. Today*, **21**, 505 (1994).

Arena, F., F. Frusteri, A. Parmaliana, and N. Giordano, ''Temperature Programmed Reaction: A Powerful and Reliable Method for Catalyst Testing in the Partial Oxidation of Methane to Formaldehyde,'' *Appl. Catal. A: General*, **125**, 39 (1995).

Arena, F., N. Giordano, and A. Parmaliana, ''Working Mechanism of Oxide Catalysts in the Partial Oxidation of Methane to Formaldehdye. Part II,'' *J. Catal.*, **167**, 66 (1997).

Arena, F., F. Frusteri, and A. Parmaliana, ''Modeling the Partial Oxidation of Methane to Formaldehdye on Silica Catalyst,'' *Appl. Catal. A: General*, **197**, 239 (2000).

Bielañski, A., and J. Haber,'' *Oxygen in Catalysis*, Dekker, New York (1991).

Brown, M. J., and N. D. Parkyns, ''Progress in the Partial Oxidation of Methane to Methanol and Formaldehyde,'' *Catal. Today* **8**, 305 (1991).

Faraldos, M., M. A. Bañares, J. A. Anderson, H. Hu, I. E. Wachs, and J. L. G. Fierro, ''Comparison of Silica-Supported MoO_3 and V_2O_5 Catalysts in the Selective Partial Oxidation of Methane,'' *J. Catal.*, **160**, 214 (1996).

Herman, R. G., Q. Sun, C. Shi, K. Klier, C.-B. Wang, H. Hu, I. E. Wachs, and M. M. Bhasin, ''Development of Active Oxide Catalysts for the Direct Oxidation of Methane to Formaldehyde,'' *Catal. Today*, **37**, 1 (1997).

Kartheuser, B., B. K. Hodnett, H. Zanthoff, and M. Baerns, ''Transient Experiments on the Selective Oxidation of Methane to Formaldehyde over V_2O_5/SiO_2 Studied in the Temporal-Analysis-of-Products Reactor,'' *Catal. Lett.*, 21, 209 (1993).

Kasztelan, S., ''Rate of Heterogeneous Catalytic Reaction Involving Ionic Intermediates,'' *Ind. Eng. Chem. Res.*, **31**, 2497 (1992).

Kennedy, M., A. Sexton, B. Kartheuser, E. Mac Giolla Coda, J. B. McMonagle, and B. K. Hodnett, ''Selective Oxidation of Methane to Formaldehyde: Comparison of the Role of Promoters in Hydrocarbon Rich and Lean Conditions,'' *Catal. Today*, **13**, 447 (1992).

Koranne, M. M., J. G. Goodwin, and G. Marcelin, ''Carbon Pathways for the Partial Oxidation of Methane,'' *J. Phys. Chem.*, **97**, 673 (1993).

Koranne, M. M., J. G. Goodwin, and G. Marcelin, ''Oxygen Involvement in the Partial Oxidation of Methane on Supported and Unsupported V_2O_5,'' *J. Catal.*, **148**, 378 (1994).

Kung, H. H., ''Kinetic Analysis of a Generalized Catalytic Selective Oxidation Reaction,'' *J. Catal.*, **134**, 691 (1992).

Mauti, R., and C. A. Mims, ''Oxygen Pathways in Methane Selective Oxidation over Silica Supported Molybdena,'' *Catal. Lett.*, **21**, 201 (1993).

McCormick, R. L. G. O. Alptekin, A. M. Herring, T. R. Ohno, and S. F. Dec, ''Methane Partial Oxidation over Vanadyl Pyrophosphate and the Effect of Fe and Cr Promoters on Selectivity,'' *J. Catal.*, **172**, 160 (1997).

Parmaliana, A., F. Frusteri, A. Mezzapica, D. Miceli, M. S. Scurrell, and N. Giordano, ''A Basic Approach to Evaluate Methane Partial Oxidation Catalysts,'' *J. Catal.*, **143**, 262 (1993).

Parmaliana, A., V. Sokolvskii, D Miceli, F. Arena, and N. Giordano, ''On the Nature of the Catalytic Activity of Silica-Based Oxide

Catalysts in the Partial Oxidation of Methane to Formaldehyde with O_2,'' *J. Catal.*, **148**, 514 (1994).
Parmaliana, A., F. Arena, V. Sokolovskii, F. Frusteri, and N. Giordano, ''A Comparative Study of the Partial Oxidation of Methane to Formaldehyde on Bulk and Silica Supported MoO_3 and V_2O_5 Catalysts,'' *Catal. Today*, **28**, 363 (1995a).
Parmaliana, A., V. Sokolovskii, D. Miceli, F. Arena, and N. Giordano, ''On the Nature of the Active Sites of Silica Based Oxide Catalysts in the Partial Oxidation of Methane to Formaldehye,'' *Catal. Today*, **24**, 231 (1995b).
Parmaliana, A., and F. Arena, ''Working Mechanism of Oxide Catalysts in the Partial Oxidation of Methane to Formaldehyde. Part I,'' *J. Catal.*, **167**, 57 (1997).
Paramaliana, A., F. Arena, F. Frusteri, and N. Mondello, ''High Yields in the Catalytic Partial Oxidation of Natural Gas to Formaldehye: Catalyst Development and Reactor Configuration,'' *Stud. Surf. Sci. Catal.*, **119**, 551 (1998).
Sokolovskii, V., ''Principles of Oxidative Catalysis on Solid Oxides,'' *Catal. Rev.-Sci. Eng.*, **32**, 1 (1990).
Spencer, N. D., and C. J. Pereira, ''Partial Oxidation of CH_4 to HCHO over a MoO_3-SiO_2 Catalyst: A Kinetic Study,'' *AIChE J.*, **33**, 1808 (1987).
Spencer, N. D., and C. J. Pereira, ''V_2O_5-SiO_2-Catalyzed Methane Partial Oxidation with Molecular Oxygen,'' *J. Catal.*, **116**, 399 (1989).
Sun, Q., R. G. Herman, and K. Klier, ''Selective Oxidation of Methane with Air over Silica Catalysts,'' *Catal. Lett.*, **16**, 251 (1992).
Vikulov, K., G. Martra, S. Coluccia, D. Miceli, F. Arena, A. Parmaliana, and E. Paukshtis, ''FTIR Spectroscopic Investigation of the Active Sites on Different Types of Silica Catalysts for Methane Partial Oxidation to Formladehyde,'' *Catal. Lett.*, **37**, 235 (1996).

Manuscript received Nov. 8, 1999, revision received Apr. 17, 2000.